IoMT-enabled stress monitoring in a virtual reality environment and at home

Luis M. Vela, Henry Crandall, Taehwan Lim, Fu Zhang, Austin Gibbs, Andrew R. J. Mitchell, Adrian Condon, Lisa M. Diamond, Huanan Zhang, and Benjamin Sanchez, *IEEE Senior Member*

***Abstract*—*Objective:* Modern lifestyles are triggering stress at a disproportionate rate for longer periods of time. Chronic or long-lasting stress can pose a risk to our health. Despite advances in physiological recording methods, mental stress remains challenging to quantify and monitor. *Methods:* We describe an Internet of Medical Things (IoMT) device with electrocardiogram (ECG) recording features. The recorded ECG signal is processed on-the-fly to calculate, in real time, heart rate, heart rate variability, energy expenditure and mental stress. Data are sent to an online platform using a standard Internet of Things (IoT) publish-subscribe messaging transport protocol for continuous monitoring. *Results:* The system functionality is first validated by performing hardware-in-the-loop measurements connected to a patient simulator. We then monitored induced stress by recording ECG in subjects using liquid metal electrodes performing a plank walking task in a virtual reality (VR) environment with high heights exposure. The results demonstrate our IoMT system's ability to provide accurate ECG metrics using novel liquid metal electrodes by detecting continuously increased stress values in a VR setting and at-home. *Conclusion:* The IoMT measurement device presented provides a novel strategy for monitoring stress in real time. *Significance:* Our work provides the opportunity for future research on psychological stress and emotion regulation within daily life and the physiological mechanisms through which it influences the health of both children and adults.**

***Index Terms*—Internet of Medical Things (IoMT), electrocardiogram (ECG), heart rate (HR), stress, liquid metal electrodes.**

I. Introduction

PSYCHOLOGICAL stress is a complex psychobiological phenomenon that occurs when individuals encounter environmental demands that exceed their resources for meeting these demands [1]. Stress activation triggers a complex chain of physiological events commonly referred to as the "*fight or flight*" response, evolved to facilitate human survival in the face of acute physical danger, but it takes a long-term toll on human health. Specifically, cumulative wear and tear across the total complex of stress-regulatory systems, typically described as allostatic load [2], [3], has deleterious health consequences [4], [5]. Hence, capturing the dynamic process of stress-regulation as it unfolds within daily life has been a chief goal of health psychologists investigating the biological mechanisms of stress and long-term health.

L. M. Vela is with the Department of Automotive Electrical Systems at Kostal Electrica S. A. C/Notari Jesus Led num. 10, Pol. Ind. Can Clapers, Sentmenat 08181, Barcelona, Spain.

F. Zhang is with the College of Engineering and Design, Hunan Normal University, Changsha 410081, China.

A. Condon is with B-Secur, Ltd., Catalyst Inc, The Innovation Centre Queen's Road, Belfast, BT3 9DT, UK.

T. Lim and H. Zhang are with the Bioelectronic Interface Research Lab, Department of Chemical Engineering, University of Utah, Salt Lake City, Utah 84112, USA.

L. M. Diamond is with the Department of Psychology, University of Utah, Salt Lake City, Utah 84112, USA.

A.R.J. Mitchell and A. Gibbs are with the Allan Lab, Jersey General Hospital, Jersey JE1 3QS, Jersey.

H. Crandall and B. Sanchez are with the Department of Electrical and Computer Engineering, Sorenson Molecular Biotechnology Building, Office 3721, 36 S. Wasatch Drive, University of Utah, Salt Lake City, Utah 84112, USA, Phone: (801)-585-9535. Corresponding author's email: benjamin.sanchez@utah.edu

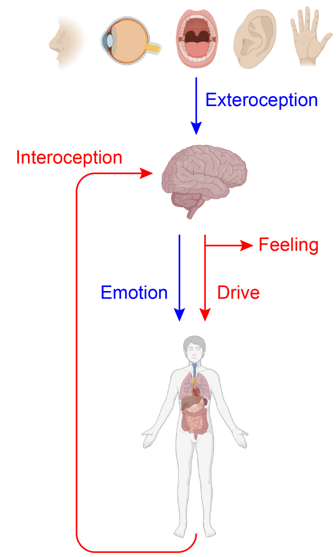

Fig. 1. Schematic of the sensitivity to stimuli outside the human body, also known as exteroception, and our felt experience of the internal workings of the human body known as interoception, affecting our emotions and stress in particular.

Current studies postulate that external stimuli act on the cortex and generate an autonomic action, also known as emotions, including stress [6]. It is then the awareness of those physiological changes and the sensory input that results in the feelings that we describe (see Figure 1). Yet capturing stress-regulation has proven challenging. Typically, researchers bring subjects into laboratories and observe their behavior and physiology as they undergo naturalistic social interactions [7]–[15]. During these interactions, subjects are typically wired to benchtop equipment for comprehensive psychophysiological assessment of autonomic nervous system functioning (heart rate –HR– derived from the electrocardiogram, blood pressure, heart rate variability –HRV–, respiration, or electrodermal activation).

Scientists uniformly acknowledge that patterns of physiological reactivity observed during laboratory-based interactions including stress may not generalize to the real world out-of-the-lab context, given the artificiality of the laboratory environment and the participants' ongoing awareness of being observed.

However, measuring stress during realistic out-of-the-lab interactions has been limited due to challenges related to a lack in wearability, accuracy, and reliability of existing devices. Indeed, only one published study has directly compared autonomic reactivity during laboratory-based and home-based interactions using the same equipment (ambulatory assessment of electrocardiogram using wearable electrodes) [16]. The authors found significantly greater HR reactivity during the home assessment than during the laboratory assessment, suggesting that participants might be editing their behavior in the laboratory in a socially desirable direction.

Current and emerging wearable Internet of Medical Things (IoMT) devices provide an effective opportunity to solve this problem [17]. Cost affordable, open source hardware and software development platforms like Raspberry Pi, Beaglebone and Arduino can be used to develop state-of-the-art wearable IoMT devices for continuous electrocardiographic (ECG)-based stress monitoring [18]. However, achieving adoption of IoMT devices requires easy-to-use technology and thus devices that rely on a computer or smartphone running off-line data processing algorithms do not provide an optimal solution.

Here, we describe a fully software embedded IoMT ECG-based device for continuous beat-to-beat monitoring of HR, HRV, energy expenditure and mental stress (Figure 2). The latest system integrates a newer analog front end version based on our recently developed IoMT platform [19]. We describe and characterize the ECG signal chain as well as the new ECG and IoMT functionalities. In addition, we built and characterized conductive polymer encapsulated liquid metal electrodes for uninterrupted ECG recording. Finally, we validate the system and liquid metal electrodes by performing continuous lab-based and home-based monitoring of stress.

II. Materials

A. System description

An overview of the up-to-date system functionality developed at the University of Utah is shown in Figure 2. The hardware device is based on the commercially available Red Pitaya platform, which integrates a System-on-Chip (SoC) Zynq-7010 (Xilinx, Inc., San Jose, CA). The SoC combines ARM dual-core Cortex-A9 MPCore processors with a field programmable gate array (FPGA), analog-to-digital converter (ADC) LTC2145 (125 Ms s^{-1}, 14 bits, Analog Devices, Inc., Norwood, MA, USA), and digital-to-analog converter (DAC) AD9767 (125 Ms s^{-1}, 14 bits, Analog Devices, Inc.). The system's size footprint is 107×60×21 mm (length × width × height) and is powered by an AC/DC adapter. The high-speed ADC and DAC channels on the Red Pitaya interface with our new analog front end (AFE) circuitry explained below. The input voltage is 5 V and the maximum and nominal power consumption are 2 A and <0.9 A, respectively.

B. Hardware

The new hardware architecture of the developed AFE, shown in Figure 3, now supports up to 16 impedance channels and one biopotential channel for ECG measurement. The AFE includes two DB15 ports to connect the electrode cables for impedance and ECG measurements, while the expansion connectors on the middle are used to provide power supply to the AFE board, generate high-speed digital signals for impedance control, and acquire the ECG signal.

Compared to our previous impedance AFE [19], the new AFE bioimpedance signal chain includes a mirrored current source (AD830, Analog Devices, Inc.), a differential amplifier and a total of four 16-to-1 multiplexers (ADG1406, Analog Devices, Inc.) for impedance measurements. The bioimpedance current and voltage signals from the ADC and DAC are filtered with 50 Ω low-pass filters from DC to 3 MHz (SXLP-3+, Mini-Circuits, Brooklyn, NY).

The biopotential AFE for ECG measurements tested in this work is based on TLV245x amplifiers (Texas Instruments, Inc., Dallas, TX) operating with a single power supply (3.3 V). It uses a driven right leg circuit to offset the subject's body to a DC common mode voltage, centering the biopotential signals with respect to the amplifier's input voltage range. The 3-lead ECG AFE is configured with a gain of 60 dB (1000) distributed in three stages with gains of 10, 20 and 5 in the first, second and third stages, respectively. The DC input range was set to ±200 mV. The bandwidth ranges from 0.05 Hz to 10 kHz and the common mode rejection ratio is 126 dB at 50 Hz [20].

C. Software

The architecture of the implemented embedded software is presented in Figure 4. The Zynq system-on-chip device runs the software application on a Linux operating system that controls the ARM-based processor and the firmware application which defines the FPGA configuration for DAC generation and ADC acquisition. The software is a multi-thread application using circular buffers as inter-process communication mechanisms (IPC), which allow us to increase modularity and code re-usability for future development. The application runs five different user-level threads: (1) ADC impedance data acquisition, (2) impedance data processing and calculation, (3) ADC biopotential data acquisition, (4) algorithm calculation and (5) Internet of Things (IoT) data management. Below the user layer, there is a service layer handling data persistence, remote web access, digital signal processing services, self-test monitoring processes, FPGA data and configuration interface, and finally, the low level microcontroller abstraction layer (MCAL) handling the drivers for network communications, memory media and ADC/DAC modules.

The structure of our architecture is based on C-language code and libraries running on embedded Linux. The web access is provided by an NGINX open source web server (NGINX, Inc., San Francisco, CA, USA). This web access allows the user to configure measurement parameters and visualize in real-time both impedance and ECG signal data processing requiring high bandwidth. The NGINX server uses

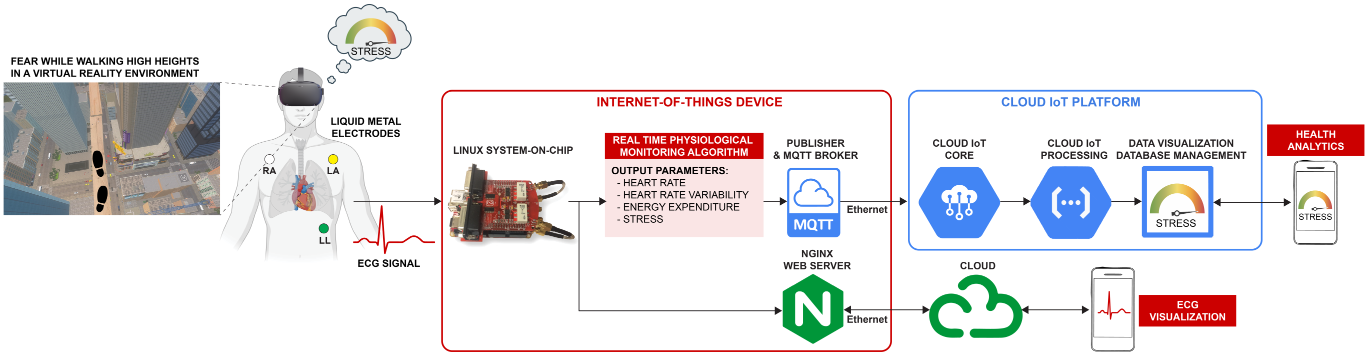

Fig. 2. System functionality of the materials, device and algorithms developed.

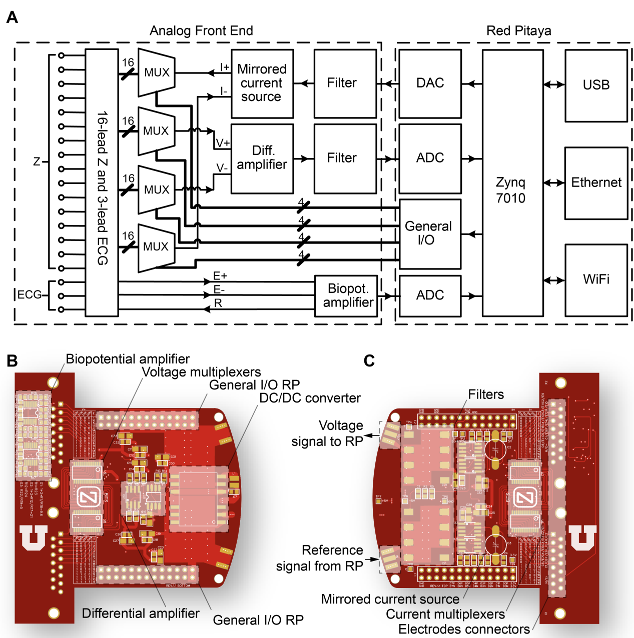

Fig. 3. (A) Overview of the hardware architecture. (B) Bottom and (C) top views of the custom built analog front end (AFE). The system is based on the Red Pitaya (RP) development board and a 16-channel AFE for bioimpedance (Z) and electrocardiogram (ECG) measurement. The Ethernet and WiFi peripherals are used for RP Internet communication and the USB bus is for system maintenance and debug. The current excitation for Z measurement is generated in the RP with the digital to analog converter (DAC) connected to a mirrored current source in the AFE. The impedance voltage signal is filtered, then conditioned with a differential amplifier, and finally measured with an analog-to-digital (ADC) converter in the RP board. The biopotential amplifier is used to acquire ECG signals at the same time that Z is measured. Abbreviations: $I\pm$ and $V\pm$, differential current and voltage signals for bioimpedance measurement, respectively; $E\pm$, differential voltage signals for ECG measurement; R, reference signal for ECG measurement; Z, multi-channel electrodes for bioimpedance measurement; MUX, multiplexers; USB, universal serial bus; WiFi, wireless fidelity; I/O, input/output; DC, direct current.

a shared object library containing the functional features. Inside this library POSIX-threads are used to create the multi-thread environment, together with mutex artifacts to manage resource access from the threads. Using a customized application programming interface the software can access the FPGA firmware. Low level drivers, data persistence and other tasks are directly managed by the Linux kernel.

D. ECG algorithm

We used the Heartkey algorithm (B-Secur, Ltd., Belfast) to process the 3-lead ECG signal in real time (see Figure 5). Figure 6 shows the main stages, described below.

1) Signal conditioning: The signal conditioning module is the initial step in processing acquired ECG samples. The aim of this stage is to identify and remove noise from the raw signal. It is common that noise in the forms of power line frequency (50 or 60Hz depending on the geographic region), muscle noise, motion and baseline wander (low frequency artifact) are present on the signal. This is accomplished through two main stages: (1), Signal Quality Analysis Stage for signal processing and noise annotation; and (2), Pre-Processing including filtering the signal. Within the first Analysis Stage, leads on/off Status and other noise events are checked. To reduce noise and ensure the signals of the desired ECG frequency range are passed through the higher processing stages, the signal enters the Pre-Processing stage. This stage comprises a number of filtering stages including high pass/low pass and notch filters. The two stages work together to produce filtered ECG samples suitable for waveform analysis.

The QRS Detection and Analysis modules take the filtered ECG samples as an input and identifies the location of the QRS complex. QRS detection is based on a real time QRS location technique which involves further filtering of the ECG signal to extract the QRS component of the ECG. The analysis involves examining each beat and making a decision on whether it is a genuine beat or in band noise.

The next stage is the RR interval module. The primary responsibility of this module is to calculate the valid RR interval series, which is defined as the time between a peak and the previous peak. In addition to reporting the time between R peaks, the RR calculation also contains an outliers removal function to ensure any misidentified noise peaks are detected and removed in noisy RR series. Outliers are removed to ensure that the calculated RR intervals are valid and within an expected range.

2) Heart rate: The HR algorithm is designed to detect heart rates in the range of 30 beats per minute (20 ms RR interval) to 300 beats per minute (2000 ms RR interval). Thus, any intervals outside these limits are rejected. The last nine RR intervals which pass the above checks will be stored, and the median value used to calculate the HR. Once nine intervals

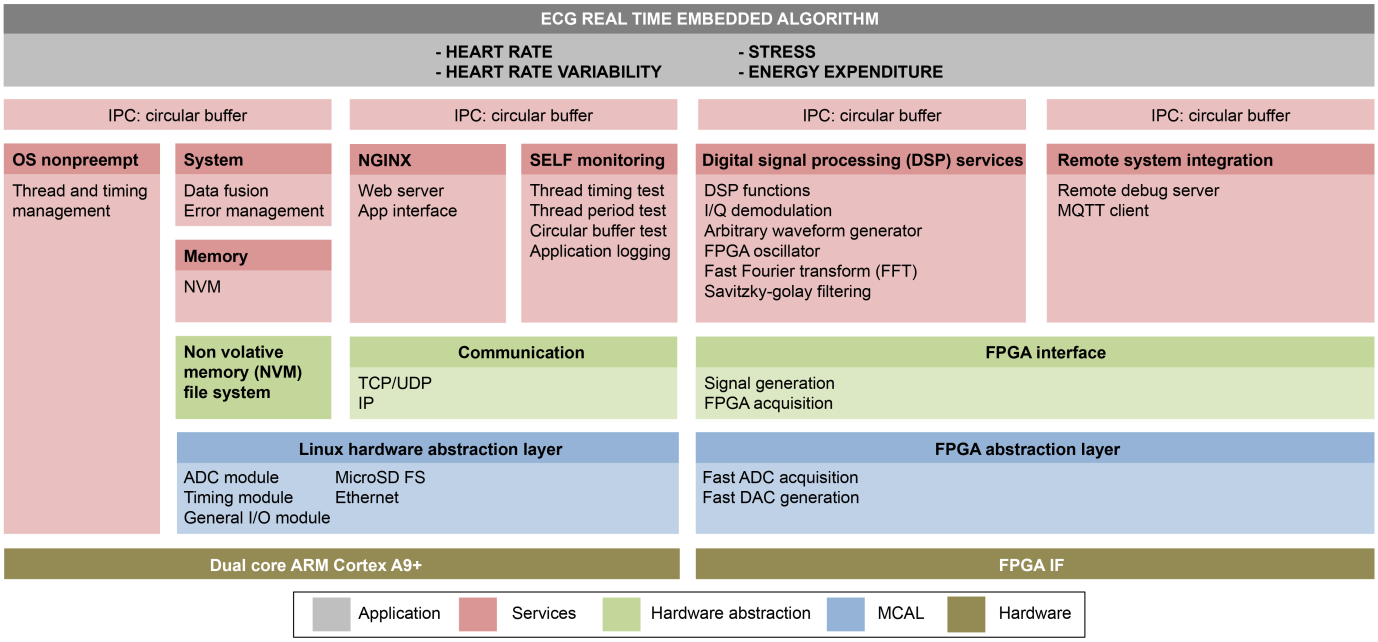

Fig. 4. Overview of the embedded software architecture. Abbreviations: MCAL, microcontroller abstraction layer; ADC, analog to digital converter; DAC, digital to analog converter; FPGA, field programmable gate array; OS, Linux operating system; IPC buffer, inter-process communication buffer.

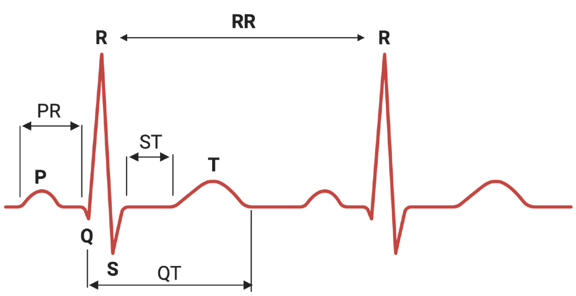

Fig. 5. A basic electrocardiogram waveform. Heart rate variability (HRV) is the fluctuation in time between two consecutive heart beats, as determined by the RR segment. HRV is associated with impaired regulatory and homeostatic autonomic nervous system functions, which reduce the body's ability to cope with internal and external stressors (see Figure 1).

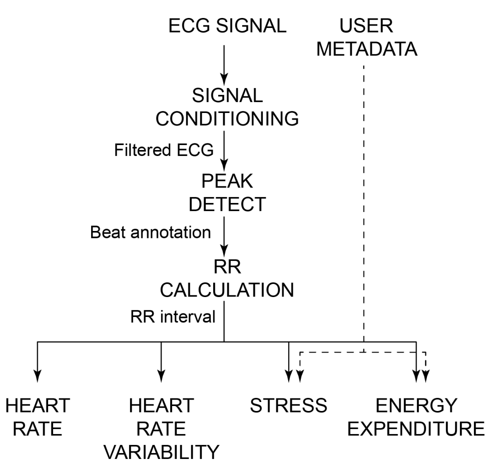

Fig. 6. Overview of the electrocardiogram (ECG) signal processing module. The acquired ECG signal is first pre-conditioned to reduce noise interference. Filtered ECG data is then analyzed to detect QRS complexes, annotate beats and calculate heart rate, heart rate variability from RR intervals, energy expenditure and stress.

are available an accuracy flag is set and the progress is 100%.

3) Heart rate variability: The algorithm measures HRV, including the root mean square of the successive differences and standard deviation of the RR Series. The algorithm calculates the HRV over a 30 second interval and will reset the HRV calculation if the following events occur: User Not Present or no RR intervals received for a period of 2.5 minutes.

4) Stress: The Stress feature requires RR interval, HRV data and MetaData information from the user (gender, age, weight, and height). The library will measure the stress value of the user as a value from 0 to 100 and will calculate the stress over a 30 second interval (i.e., latency).

5) Energy expenditure: This algorithm considers the user's physiological data while utilizing HR and HRV measurements against time to detect changes in an individual's energy demands. The algorithm outputs a value in the form of kilocalories per minute. Energy expenditure values are calculated on an accumulation basis and displayed for that individual. The algorithm provides active energy expenditure (e.g., energy burnt during activities such as walking and running) and rest energy expenditure (i.e., baseline metabolic energy consumed by the body).

E. Internet of Things communication protocol

IoT communication is performed using the message queuing telemetry transport protocol (MQTT). The application relies on the Paho MQTT-C client implementation. This code is dynamically linked using a shared object and provides encrypted MQTT connectivity. MQTT protocol is used to send beat-to-beat HR (in beats per minute), HRV, energy expenditure and stress data periodically as well as other system status information. In our software application, the type of information, topics, period and other configuration parameters were adapted to the IoT Kaaiot server.

III. METHODS

A. Liquid metal electrodes

Liquid metal electrodes of dimensions 2 cm×2 cm×0.2 mm were fabricated using Eutetctic Gallium Indium (EGaIn, ≥99.99% trace metals basis, Sigma-Aldrich, Inc., St. Louis, MO) and polydimethylsiloxane (PDMS, 250 μm thickness (Stockwell Elastomerics, Inc., Philadelphia, PA). The electrode consisted of the liquid metal encased by two layers of PDMS. The bottom PDMS surface was treated using O_2 plasma treatment for five minutes to improve the spread of EGaIn. The total thickness of the liquid metal sheet sandwiched by the PDMS films is 700 μm. The electrode site was prepared by removing a 4 mm diameter hole at the center of the top PDMS layer. Poly (3,4-ethylene dioxythiophene) (PEDOT) was electrodeposited using a potentiostat (SP-150, Bio-logic, France) with a three-electrode system. Platinum and silver/silver chloride wires were used as the counter and reference electrodes, respectively.

First, gold nanoparticles were deposited on the exposed liquid metal surface by electrochemical deposition. Aqueous gold solution was prepared from 0.2 mM gold (III) chloride hydrate (Hydrogen tetrachloroaurate hydrate, HAuCl4, 99.999%, Acros organics, USA) and 0.1 M potassium chloride (KCl, 99.5%, Sigma-Aldrich) [21]. The electrochemical deposition was performed using a negative potential ($Au^{3+} + 3e^{-} \rightarrow Au$) to prevent the formation of an oxide layer and provide a uniform electrical field on the liquid metal. The deposition was conducted from -2.0 V for 10 minutes to guarantee uniform coating with 500 nm thickness on the entire liquid metal surface.

Next, biocompatible PEDOT was prepared from the non-aqueous electrolyte, propylene carbonate (PC, anhydrous, 99.7%). Tetraethylammonium tetrafluoroborate (TEABF4, 0.12 M, 99%) was selected as a suitable dopant, which is non-soluble in a water-dominant environment but dissolves in the PC electrolyte. The PEDOT was polymerized from ethylene-dioxythiophene (EDOT, 97%) by an electrochemical reaction with an anodic current of +1.3 V for 10 minutes. Following polymerization, the PEDOT was doped by tetrafluoroborate. Finally, the PEDOT was deposited on the gold nanoparticles layer to improve biocompatibility.

B. Electrical impedance characterization of liquid metal electrodes

Impedance measurements of liquid metal electrodes were performed in phosphate buffered saline (1xPBS, pH 7.4, GibcoTM), a popular physiologic electrolyte to confirm the electrochemical properties of the bioelectronics. Bode plots were generated from electrical impedance measurements in the frequency range between 10 Hz and 0.1 MHz with a 20 mV sinusoidal amplitude. A three-electrode electrochemical cell system was prepared and evaluated using a potentiostat (SP-150, Bio-logic, France) with EC-Lab V11.10 software. The liquid metal electrodes were connected to the working electrode. Stainless steel mesh (50x50 mm^2) and Ag/AgCl electrode were used as the counter and reference electrodes, respectively.

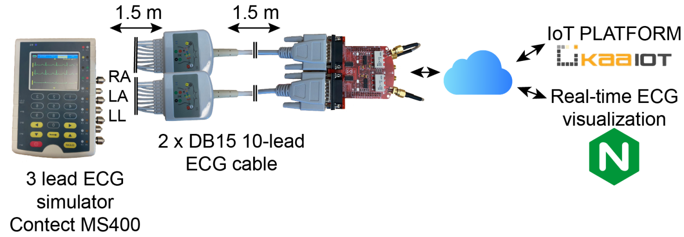

Fig. 7. Three lead electrocardiography (ECG) hardware-in-the-loop setup. The device is connected to the patient simulator (Contect MS400) using 10-lead ECG cables and to the Internet via an Ethernet connection. The device is controlled in real time by remote access through the user interface provided by NGINX web server. Abbreviations: RA, right arm; LA, left arm; LL, left leg.

C. Electrodes ECG test fixture

We developed a reference electrode characterization setup to test the liquid metal electrodes measuring finger-based ECG (Figure 9 A). The system consists of electronic hardware for ECG acquisition linked to a Bluetooth module. The acquired ECG signal, via the liquid metal electrodes, is transmitted to an Android device where the ECG signal and ECG-derived metrics are plotted and analyzed by an Android application (Figure 9 B). These metrics are heartbeat detection (number of heartbeats expected and detected), RR interval detection (number of RR intervals expected and detected), and time to first beat detected, the latter a measurement that provides insight into how quickly the electrode material can acquire a signal. As part of testing for an ECG electrode use case, the liquid metal electrodes were placed in the test fixture and then both index fingers were inserted into the left and right finger mounts touching the liquid metal electrodes. A third wet electrode was connected to the wrist using the right-leg drive connector.

D. Hardware-in-the-loop testing

Figure 7 shows the hardware-in-the-loop (HIL) setup used to develop and test our real-time IoMT embedded system. A three lead ECG patient simulator (Contect MS400) was used to emulate a real patient in order to simulate a controllable reference ECG signal. The ECG signal was sent to our system using 3 m long 10-lead ECG cables. The system was connected to the Internet with an Ethernet cable to provide the user access to the NGINX web server and IoT connectivity. For the HIL experiments, the ECG signal beats per minute was manually changed to test the overall system functionality to acquire and process, in real time, the ECG signal, detect QRS complexes and calculate HR, HRV, energy expenditure and stress data.

E. ECG analysis performance

1) ECG data collection in a motion based protocol: The ECG data collection protocol using a motion based protocol consisted of (i), one minute resting baseline while sitting upright; (ii), one minute light walk followed by one-minute brisk walk; and (iii), one minute resting recovery while standing. Note the optimal ECG data collection method involves subjects in stationary position. Thus, this protocol is intentionally challenging as it involves varying levels of motion to represent realistic out-of-the-lab ECG collection conditions including the presence of motion artifacts which may arise. ECG data for the motion protocol was acquired and compared to an FDA-cleared ECG recording device and associated analysis software (Faros 180, Bittium Corporation, Oulu, Finland). For convenience and availability, we used commercial gel-adhesive electrodes (BlueSensor, Ambu). A total of 14 subjects (29.5 ± 6.5 years) were measured.

- *ECG signal processing*. Three ECG signals were collected and processed to produce real time HR. ECG signals were also processed by the associated software provided alongside the Holter monitor and used as the ground truth.
- *Data analysis*. The average and the mean difference of the HR was plotted against the ground truth using Bland-Altman graphs and compared to the American National Standards Institute EC13 standard for proof-of-concept validation.

2) Benchmark comparison: The ability of the HeartKey algorithm to successfully detect the QRS complex amidst various levels of noise was determined using three PhysioNet databases publicly available: the MIT-BIH database, the AHA database, and the ESC (ST-T) database.

F. Stress-induced in a virtual environment by fear of high heights

We exposed subjects to a stress-inducing environment by using virtual reality goggles (Oculus Quest 2, Irvine, CA) to mimic performing a plank walk on the roof of a skyscraper (Plank not included, 4 Fun Studio, Inc.). The subject did not have any experience with the virtual reality equipment prior to the study. In addition, the perceived experience was enhanced by having subjects stand with their feet on a wooden plank. During the virtual reality activity, an ECG was recorded using liquid metal electrodes (Section III-A) and HR, HRV, energy expenditure and stress were transmitted to an IoT cloud server. The right and left arm electrodes were placed under the right and left clavicles, respectively, at the mid-clavicular line within the rib cage frame; and the leg electrode on the lower left abdomen within the rib cage frame. This study was approved by the Institutional Review Board of the University of Utah (protocol number 00144572).

IV. Experimental results

A. Liquid metal electrodes characterization

1) Electrode impedance on phosphate buffer saline solution: The bare liquid metal surface featured a smooth structure that typically delivers high (worse) electrode impedance than other structures such as porous or rough surfaces due to a limited effective electrode surface area. The multi-frequency data indicate the bare liquid metal surface had an impedance of approximately 6 kΩ at 100 Hz, which is a representative frequency for ECG recordings. Surface modification was performed to improve biocompatibility of the liquid metal electrodes using gold nanoparticles and PEDOT. Both layers produced rough and nano-porous structures on the liquid metal surface, resulting in a lower impedance: 300 Ω after gold nanoparticles deposition and 100 Ω after PEDOT deposition. The final liquid metal-based electrodes provide wearing comfort and high electrochemical performance (reduced electrode impedance) for ECG recordings.

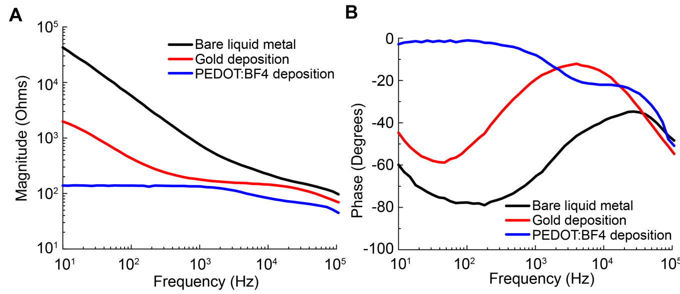

Fig. 8. Electrical impedance spectroscopy characterization results of the poly (3,4-ethylene dioxythiophene)-coated liquid metal electrodes in phosphate buffered saline solution compared to bare liquid metal and gold deposition only.

2) Biopotential recording of finger-based ECG signals using liquid metal electrodes: The liquid metal electrodes' performance recording ECG signals was tested using the developed electrode test fixture. An illustrative finger-based ECG recoding with liquid metal electrodes is shown in Figure 9 B. The included animation video in the Supplementary Multimedia material is a demonstration of the test electrode jig measuring finger to finger. The displayed tracing of the corresponding measurement is the resultant ECG signal. At the completion of the test, the test file includes the time to first heartbeat detected, the number of heartbeats detected, and the number of RR intervals detected.

B. Hardware-in-the-loop verification

The verification test results presented in Figure 10 and 11 were performed using the hardware-in-the-loop approach interfacing our newly developed system to an ECG patient simulator. Figure 10A shows the raw ECG signal acquired continuously in the web browser by accessing the NGINX server prior to processing. This signal is processed by the embedded Heartkey algorithm to compute, in real time, the HR, shown in Figure 10B (80 beats per minute). Figure 11 shows continuous HR, HRV, energy expenditure and stress data transmitted using MQTT to an IoT cloud server over a 3 minute window. During this time, we manually changed the HR of the patient simulator in 20 beats per minute increments from 40 to 200 and vice versa.

C. ECG analysis performance

1) Noise analysis: The aim of these experiments shown in Figure 12 were to ensure the overall performance of the system at analyzing ECG data captured in the presence of varying levels of noise. The results shown in Figure 12 display how the device was able to remove baseline wander, line interference, and electrode motion noise from the ECG signal while still maintaining QRS amplitudes and morphologies.

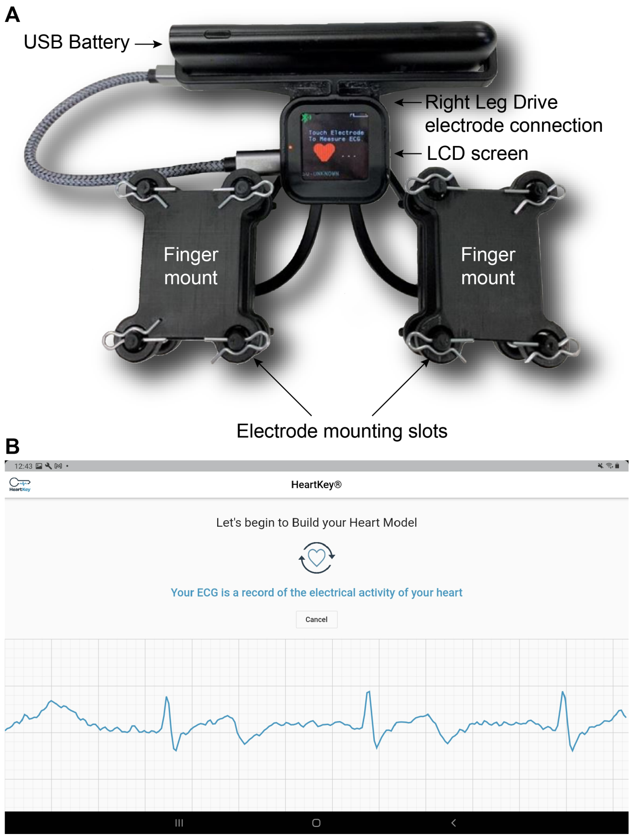

Fig. 9. (A) Electrode test fixture developed in this study to test the liquid metal electrodes for recording finger-to-finger ECG signals. The test fixture accepts electrode samples up to 25 mm x 25 mm and 0.5 to 1.5 mm in thickness. We refer the reader to the Supplementary Multimedia material for further information. (B) Finger-based ECG results using liquid metal electrodes.

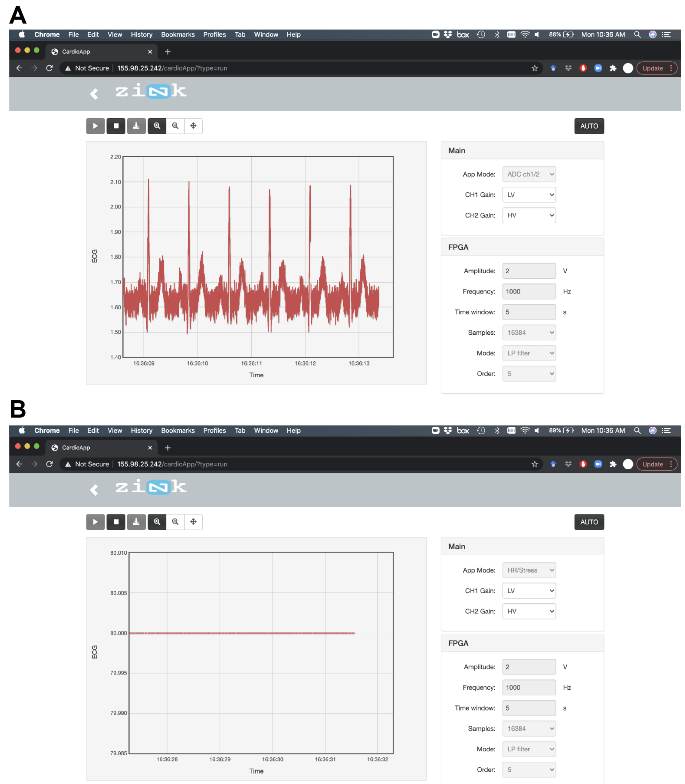

Fig. 10. Screen captures showing the NGINX web server graphical user interface developed for two different working modes while performing hardware-in-the-loop testing to validate our new platform: (A) real time electrocardiogram signal acquired with 80 beats per minute and (B) heart rate detected (80 beats per minute).

2) HR performance in a motion based protocol: Data shown in Figure 13 and quantified in Table I compare the performance against a reference FDA-cleared ECG device. Bland-Altman analysis results had an overall mean HR difference of 0.23, 0.41 and 0.44 bpm from the ground truth during each respective testing section of the motion protocol.

3) Benchmark comparison: Table II provides a comparison with selected studies that have reported the performance results of their algorithms tested in different databases. The HeartKey algorithm achieved an averaged 98.64% sensitivity and 99.69% positive predictive value for QRS detection on the three databases evaluated, which is similar to other reported algorithms that were tested in the same databases.

D. Lab-based continuous stress monitoring with the subject exposed to virtual reality high heights during a plank walk

An ECG was recorded on the participating subject using liquid metal electrodes during an 80 story high plank walk. ECG, stress and additional metrics were recorded, processed and sent in real time to an IoT cloud server as shown in Figure 14. During the plank walk, the IoMT device captured changes in the subject's HR, HRV, and stress, noting a drop in HRV while the stress levels increased.

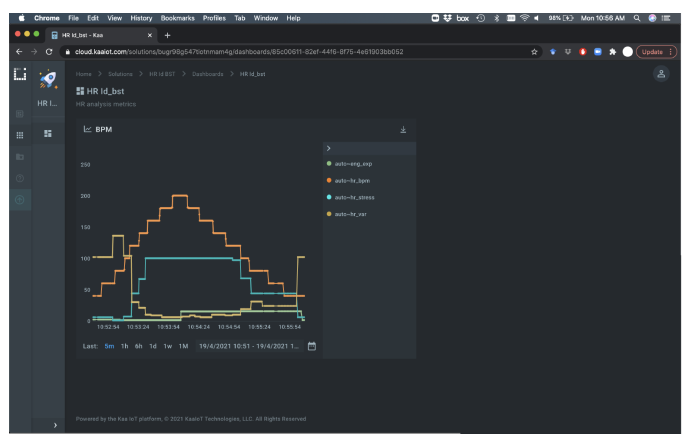

Fig. 11. Screenshot of the IoT server while performing hardware-in-the-loop measurements with the system connected to the electrocardiogram (ECG) patient simulator. Recorded results include heart rate (in beats per minute, orange), heart rate variability (yellow), energy expenditure (green), and stress (cyan) signal changes manually incrementing the rate in 20 beats per minute from 40 to 200 beats per minute and vice versa.

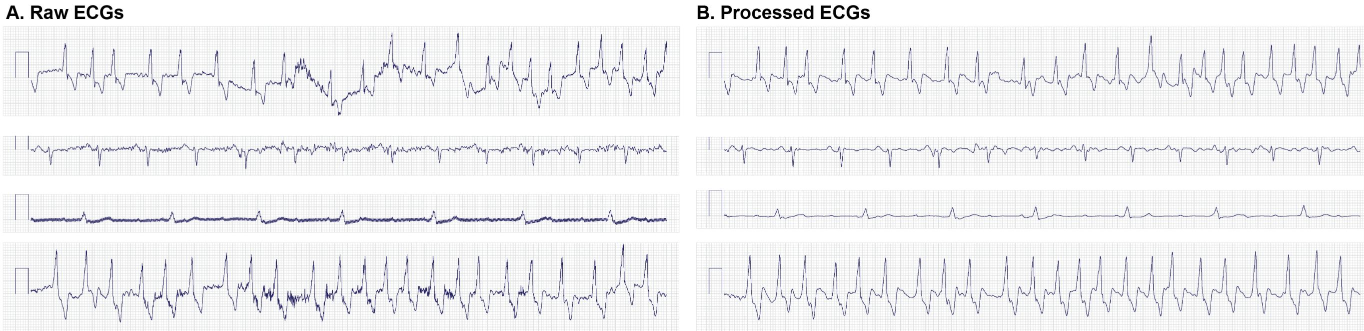

Fig. 12. (A) An ECG signal acquired including different sources of error. (B) The processed ECG with Heartkey algorithm shows the ability of our IoMT device to remove noise while maintaining the shape of the QRS complexes.

TABLE I
BLAND-ALTMAN STATISTICS AND DEVICE HEART RATE COMPARISON RESULTS FOR $N = 14$ SUBJECTS. ABBREVIATIONS: HR, HEART RATE; BPM, BEATS PER MINUTE; R, REFERENCE DEVICE; HK, HEARTKEY; CI, CONFIDENCE INTERVALS.

	Bland-Altman statistics				HR device comparison					
					HR standard deviation		Minimum HR (bpm)		Maximum HR (bpm)	
	Mean HR (bpm)	Mean HK HR (bpm)	Mean difference	Mean CI	R	HK	R	HK	R	KH
Sitting (baseline)	71	71	0.23	$-2.61, 2.64$	15.09	15.05	45	45	110	110
Walking	97	97	0.41	$-4.50, 4.04$	12.77	13.04	97	97	122	121
Standing	94	94	0.44	$-3.59, 3.48$	14.89	14.74	94	94	125	125

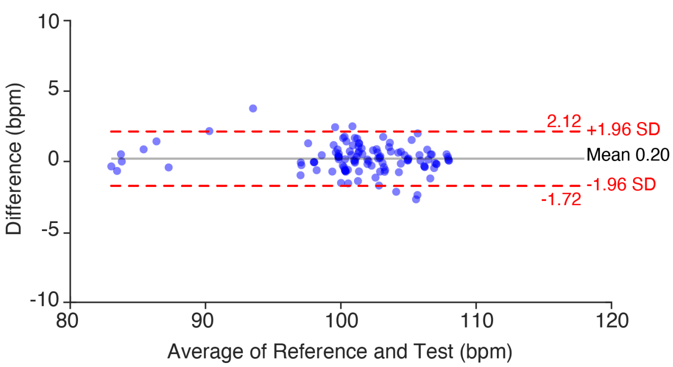

Fig. 13. Example of Bland-Altman plot from one subject comparing the heart rate detected with HeartKey against a ground truth FDA-cleared ECG device.

TABLE II
BENCHAMARK COMPARISON OF HEARTKEY QRS DETECTION AGAINST OTHER REPORTED ALGORITHMS. ABBREVIATIONS: PPV, POSITIVE PREDICTIVE VALUE; HK, HEARTKEY.

Reference	Sensitivity (%)	PPV (%)	Database
Kunzmann et al. [22]	98.96	99.86	
Iliev et al. [23]	99.86	99.73	
Tabakov et al. [24]	99.37	99.57	MIT-BIH
HK	98.96	99.86	
Kunzmann et al. [22]	97.61	99.83	
Iliev et al. [23]	99.01	99.11	
Tabakov et al. [24]	99.65	99.57	AHA
HK	97.43	99.60	
Kunzmann et al. [22]	97.21	99.90	
Iliev et al.	99.38	99.47	
Tabakov et al. [24]	99.85	99.54	ESC (ST-T)
HK	99.52	99.62	
Kunzmann et al. [22]	98.56	99.82	
Iliev et al. [23]	99.41	99.26	
Tabakov et al. [24]	99.62	99.56	Average
HK	98.64	99.69	

E. Home-based continuous stress monitoring

Figure 15 shows home-based continuous stress measurements in two subjects over a span of 24 hours. Subject A had 5 h 42 min of recovery, 14 h 4 min of low stress, 2 h 46 min of medium stress, and 1 h 17 min of high stress levels; for an averaged stress score of 35% over a 24 hours period. Subject B had a higher average stress level with a stress score of 67% and 1 min recovery, 1 h 13 min of low stress, 11 h of medium stress and 3 h 44 min of high stress.

V. DISCUSSION

A. IoMT-enabled home-based assessment of mental stress

The most widely used form of ambulatory assessment among psychologists studying everyday stress and health has been ambulatory blood pressure, which has been used to understand stress-relevant effects of marital interactions [25]–[28], broader peer and social interactions [29]–[32], and daily experiences of stress, stigma, discrimination, or social support [33]–[36]. Although blood pressure is a highly health-relevant outcome, it provides relatively limited information

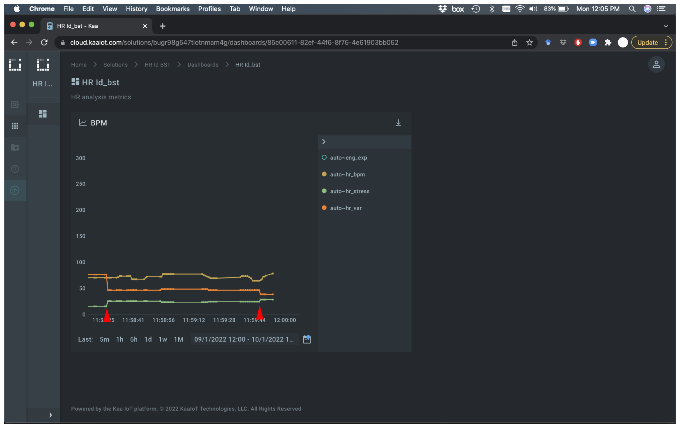

Fig. 14. Screenshot of the IoT server measuring subject's stress while exposed to virtual reality high heights during the plank walk. Arrowheads in red indicate instants of time during the plank walk where the subject's stress increased. Recorded results include heart rate (in beats per minute, yellow), heart rate variability (orange), and stress (green).

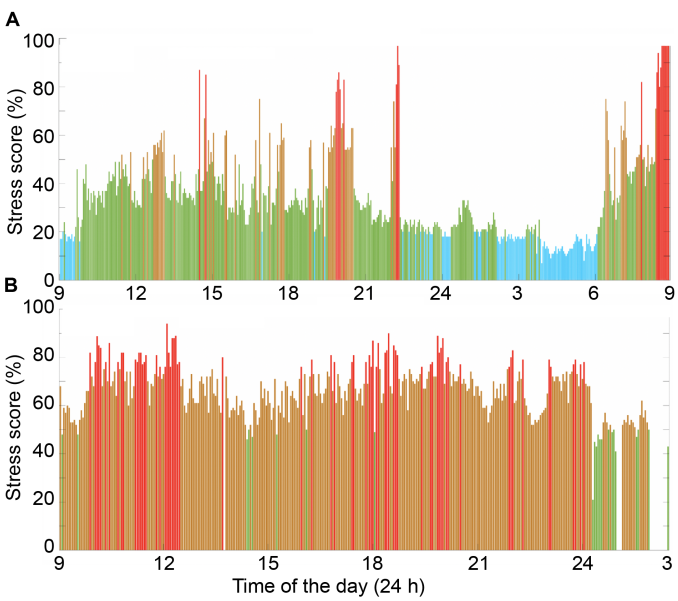

Fig. 15. Example of home-based 24-hour continuous monitoring of ECG-derived stress metrics: normal (A) and abnormal (B) score stress readings. Each colored bin corresponds to stress data averaged over a period of 5 min. In color, zones of recovery 0%<score≤20% (blue), low stress 20%<score≤50% (green), medium stress 50%<score≤80%(orange), and high stress 80%<score≤100% (red).

on the broader cascade of autonomic and endocrine physiological processes involved in day-to-day stress-regulation and emotion-regulation. Relatively few studies combine ambulatory blood pressure monitoring with salivary or plasma assessments of neuroendocrine activity [27], [37], [38]. The cumbersome nature of ambulatory blood pressure assessment is an additional (and widely acknowledged) obstacle for its use over extended periods of time, especially for children and adolescents.

For the aforementioned reason, psychologists have increasingly noted the potentially game-changing promise of IoMT technology for future research on psychological stress and emotion regulation within daily life and the physiological mechanisms through which it influences the health of both children and adults [39], [40]. Yet thus far, these promises have not yet been realized: reliability and validity of commercially available devices remains a chief concern, especially for consumer electronic products such as the FitBit, Empatica or Microsoft Band, which have not been validated as a research or clinical tool [41]. As an example, the authors in [42] found no correlation between HRV measures derived by the Empatica E4 and the same HRV measures derived from the gold standard device during slow walking or keyboard typing (Pearson correlations ranged between 0.00 to 0.07). These results were consistent with another study where the authors also concluded the Empatica E4 failed to produce reliable HRV data [43].

Here, we developed a new AFE capable of measuring ECG and implemented a real-time ECG algorithm (B-Secur, Ltd., Belfast, UK) approved by the US Food and Drug Administration. This algorithm has been clinically validated against ANSI EC57 and BS EN 60601-2-27 standards analyzing 110,000 heart beats annotated by a cardiologist and the results show a sensitivity of 99.1% and positive predictive value of 99.86%. Our results confirm the ability to report, for the first time, home-based continuous stress monitoring to an IoT cloud server.

B. ECG analysis performance

ECG signals are prone to noise contamination which can arise from 50/60 Hz power line interference, the electrode-skin interface, contact noise, and general motion artifact noise induced by the subject [44], [45]. The presence of noise artifacts within ECG signals can be particularly troublesome as they can trigger false stress values. Algorithms must then be reinforced by effective signal conditioning to ensure the processed signal is free of excess noise and thus is reflective of the true ECG signal. Effective signal conditioning will not only prevent QRS complexes being removed with noise artifacts, but it will also prevent the classification of excess noise as false QRS complexes and have a significant impact on the calculation of mental stress [46].

Our results in Figure 12 show the performance level of the HeartKey ECG software library to to obtain accurate and reliable automated detection of QRS complexes under the presence of artifacts and noise necessary to calculate HR, HRV, energy expenditure, and stress data. The results shown in Figure 13, also summarized in Table I, are within the ±10% or ±5 bpm range recommended by American National Standards Institute EC13. Despite having measured a relatively small cohort, these results suggest that our device may be effective in obtaining medical grade performance when processing in real-time out-of-the-lab ECG data simulating a challenging motion-based testing protocol.

A diverse range of algorithms have been reported in the literature tested against publicly available and annotated databases. Here, we intentionally did not include in Table II studies that specifically tested their ECG algorithm in one database only to prevent a biased comparison. The overall performance of the QRS detection on the tested database is well within the same level of performance compared to other reported algorithms. We refer the reader to our recently published work for additional results considering other databases and uses cases [47]. It is also important to consider the clinical relevance of the metrics reported in Table II and not just their numerical difference. From a clinical perspective, the impact that a sensitivity $>97\%$ would have in the "worst case" scenario with a heart rate of 200 bpm, would equal to approximately 2-3 missed or extra beats within a 30 second window, which is not deemed to be clinically significant in relation arrhythmia detection applications for example.

C. Liquid-metal-based electrodes for ECG wearable biosensing

Comfort, usability, and the ability to gather multiple data streams in a single device are particularly important for prolonged (longer than 24 hours) stress monitoring in child, adolescent and elderly populations. To address this unmet need, the research community is continuously looking for better electrode materials and for ways to better collect relevant physiological signals, including ECG [48]. There are many trade-offs including comfort, contact electrical impedance at the electrode-skin interface, and skin irritation [49]. To date, silver/silver chloride gel-adhesive electrodes are the gold standard for electrical recordings thanks to the low contact impedance between the electrode and the skin. However, long term recordings (on the order of days) can be severely affected as the gels dry out over time, thus worsening the contact impedance [50]. Dry electrodes, on the other hand, are suitable for prolonged use, but suffer from a high contact impedance, which reduces the overall signal-to-noise ratio. [51]. Extreme use cases such as continuous exposure to a demanding workload over a long period of time including athletic activities, harsh environmental conditions, and repeated use exacerbate these problems. One of the most promising materials investigated here is gallium based alloys, which has been reported to out-perform the standard wet electrode [52].

Gallium based liquid metals have emerged as a promising material for bioelectronic applications due to their intrinsic stretchability, low melting point, excellent electrical properties, and biocompatibility [53]. These unique material properties allow material scientists to fabricate stretchable and tissue-compliant bioelectronic devices [54]. However, gallium based liquid metals have limited biochemical and electrochemical stability [55], [56]. They are also prone to biodegradation in humid environments and metal leakage over time [57]. Therefore, proper chemical functionalization is necessary to ensure the liquid metal electrodes can maintain low interfacial impedance and chronic stability [58].

In this work, we have demonstrated that conductive polymer functionalized liquid metal electrodes are compliant with skin tissue and have excellent electrochemical performance enabling ECG recording to extract health parameters including HRV, and HRV-based stress, which, to the best of our knowledge, is the first time it has been reported.

D. Effects of virtual reality high heights exposure on stress

Virtual reality's ability to induce a physiological response [59]–[61] has given rise to a wide variety of useful applications including: anxiety and phobia [62], managing Post-Traumatic Stress Disorder [62], modulating pain [63] and cardiac rehabilitation [64]. In the case of generating dynamic cardiovascular responses, the work done by Ahmed et al. considered virtual reality alone, exercise alone, and exercise combined with virtual reality, with blood pressure, heart rate, and norepinephrine response as stress indicators [65]. While there was no comparable rises in virtual reality alone compared with exercise in maximal HR and norepinephrine levels, there was a comparable change in HRV, leading the authors to suggest that VR could be used to mimic moderate but not high intensity. The limitation of the chosen technology as well as the experience itself were likely confounding factors affecting the results of that study.

In this work, we explored the stress effects of high heights in virtual reality using virtual reality goggles. We leveraged the innate fear of heights to generate a stress response [66]. In previous experimental settings, [62], subjects were asked to physically walk on a balance beam while virtually at ground level or at height. Electroencephalography, cardiac physiological parameters and electrodermal activity were recorded. The authors found that the virtual reality at height decreased HRV and HR frequency when compared to virtual reality at low height. Our pilot results are consistent with previous reported results, as we detected increased stress levels during virtual high heights.

E. Limitations

The work presented here has a number of limitations. Most notably, since we measured ECG only, we were restricted to mainly studying HRV and not other common biomarkers of psychological stress, such as cortisol or electrodermal activity. Second, as noted above, the ECG was assessed while subjects walked on a plank. Future work will include a validation study of the platform and stress algorithms against the State-Trait Anxiety Index (STAI) questionnaire. This questionnaire will be used as a subjective measure of stress to assess the validity of the algorithm against an individual's own perception of their stress levels and those recorded with our device. STAI results will be tracked for each stage and correlated with participant ECG-based stress data. Multilevel models will be used to examine second-by-second correspondence between ECG data collected through the two different modalities (standard physiological equipment and our IoMT device). Third, despite the main focus of this work being to show IoMT feasibility, we acknowledge the data provided was collected on a limited number of subjects. A formal assessment of the technology will require further work and include more subjects, a comparison across multiple study sites, as well as comparison to standard laboratory equipment for the assessment of stress.

VI. Conclusions and Future directions

There is an urgent need for better and more accurate solutions to enable the population to manage their stress as it unfolds naturally, across multiple biological systems and numerous naturalistic settings. The work presented here demonstrates the feasibility of IoMT to provide an excellent platform to continuously capture the consequences of mental stress. Our results show the capability to capture health-relevant biological consequences of mental stress regulation in a controlled and repeatable way within day-to-day at home.

IoMT devices that allow the continuous monitoring of stress can be of value for a wide variety of applications, including: assessing and enhancing the performance of first responders and armed forces personnel, improving the performance of athletes, and reducing mental and physical health disparities in sexual and gender minorities. Stress training coupled with these devices can allow individuals to identify when they are becoming stressed to a critical point when performance and safety are adversely affected, and to then use techniques, such as tactical breathing, to restore proper stress levels. It is currently unclear how the measurement of stress indices can change the outcomes for these individuals, but it has been reported that many heart rhythm conditions occur in response to alterations of autonomic tone. IoMT devices will allow researchers to explore this area with greater precision to develop new preventive and therapeutic interventions for disease modification [67], [68]. It has been postulated that there may be an early change in physiological stress measurements that precedes the symptomatic changes in disease, which may be of use in predicting the health course of a patient and potential deterioration. With continuous at-home stress monitoring and AI computing [69], these potential predictive trends are being explored.

Continuous monitoring of one's physiological state can have benefits across the spectrum, from managing social life, minimizing the impact of unpleasant events, maximizing workforce wellness programs, improving performance on a weekend run, to the prediction of illness in long term health conditions. The challenge is getting the data quality and interpretation needed for accurate number. A challenge that is being met with modern IoMT devices and data science.

Conflict of Interest

Adrian Condon serves as Chief Technology Office at B-Secur, Ltd. Dr. Gibbs and Mitchell are Consultants of B-Secur, Ltd. Dr. Sanchez holds equity in Haystack Diagnostics, Inc., the company has an option to license patented technology where the author is named an inventor. He also holds equity and serves as Scientific Advisory Board Member of Ioniq Sciences, Inc. Dr. Sanchez holds equity and serves as Scientific Advisor To The Board of B-Secur, Ltd. He consults for Myolex, Inc., the company has an option to license patented technology where the author is named an inventor. Dr. Sanchez also serves as a consultant to Impedimed, Inc., the company has patented technology where the author is named an inventor. He also serve as a Consultant to Texas Instruments, Inc., Happy Health, Inc., Analog Devices, Inc, and Eko Health, Inc.

References

[1] S. Folkman, "Stress: Appraisal and Coping," in *Encyclopedia of Behavioral Medicine*. New York, NY: Springer New York, 2013, pp. 1913–1915.

[2] T. E. Seeman, B. H. Singer, J. W. Rowe, R. I. Horwitz, and B. S. McEwen, "Price of adaptation–allostatic load and its health consequences. MacArthur studies of successful aging." *Archives of internal medicine*, vol. 157, no. 19, pp. 2259–68, oct 1997.

[3] B. Singer, C. D. Ryff, and T. Seeman, "Operationalizing Allostatic Load," in *Allostasis, Homeostasis, and the Costs of Physiological Adaptation*. Cambridge University Press, oct 2004, pp. 113–149.

[4] G. W. Evans and P. Kim, "Childhood poverty and health: cumulative risk exposure and stress dysregulation." *Psychological science*, vol. 18, no. 11, pp. 953–7, nov 2007.

[5] P. J. Gianaros and T. D. Wager, "Brain-Body Pathways Linking Psychological Stress and Physical Health," *Current Directions in Psychological Science*, vol. 24, no. 4, pp. 313–321, aug 2015.

[6] A. Damasio and G. B. Carvalho, "The nature of feelings: evolutionary and neurobiological origins," *Nature Reviews Neuroscience*, vol. 14, no. 2, pp. 143–152, feb 2013.

[7] E. M. Carpenter and L. A. Kirkpatrick, "Attachment style and presence of a romantic partner as moderators of psychophysiological responses to a stressful laboratory situation," *Personal Relationships*, vol. 3, no. 4, pp. 351–367, dec 1996.

[8] L. M. Diamond, C. P. Fagundes, and M. R. Butterworth, "Attachment Style, Vagal Tone, and Empathy During Mother-Adolescent Interactions," *Journal of Research on Adolescence*, vol. 22, no. 1, pp. 165–184, mar 2012.

[9] A. Gonzalez, P. S. Moore, A. M. Garcia, M. Thienemann, and L. Huffman, "Activation During Observed Parent–Child Interactions with Anxious Youths: A Pilot Study," *Journal of Psychopathology and Behavioral Assessment*, vol. 33, no. 2, pp. 159–170, jun 2011.

[10] J.-P. Gouin, C. S. Carter, H. Pournajafi-Nazarloo, R. Glaser, W. B. Malarkey, T. J. Loving, J. Stowell, and J. K. Kiecolt-Glaser, "Marital behavior, oxytocin, vasopressin, and wound healing." *Psychoneuroendocrinology*, vol. 35, no. 7, pp. 1082–90, aug 2010.

[11] J. L. Helm, D. A. Sbarra, and E. Ferrer, "Coregulation of respiratory sinus arrhythmia in adult romantic partners." *Emotion*, vol. 14, no. 3, pp. 522–531, 2014.

[12] T. J. Loving, M. E. J. Gleason, and M. T. Pope, "Transition novelty moderates daters' cortisol responses when talking about marriage," *Personal Relationships*, vol. 16, no. 2, pp. 187–203, jun 2009.

[13] D. Murray-CloseE, A. S. Holland, and G. I. Roisman, "Autonomic arousal and relational aggression in heterosexual dating couples," *Personal Relationships*, vol. 19, no. 2, pp. 203–218, jun 2012.

[14] T. F. Robles, V. A. Shaffer, W. B. Malarkey, and J. K. Kiecolt-Glaser, "Positive behaviors during marital conflict: Influences on stress hormones," *Journal of Social and Personal Relationships*, vol. 23, no. 2, pp. 305–325, apr 2006.

[15] G. I. Roisman, "The psychophysiology of adult attachment relationships: Autonomic reactivity in marital and premarital interactions." *Developmental Psychology*, vol. 43, no. 1, pp. 39–53, jan 2007.

[16] B. R. W. Baucom, K. J. W. Baucom, J. N. Hogan, A. O. Crenshaw, S. V. Bourne, S. E. Crowell, P. Georgiou, and M. S. Goodwin, "Cardiovascular Reactivity During Marital Conflict in Laboratory and Naturalistic Settings: Differential Associations with Relationship and Individual Functioning Across Contexts." *Family process*, vol. 57, no. 3, pp. 662–678, 2018.

[17] M. S. Mahmud, H. Fang, and H. Wang, "An Integrated Wearable Sensor for Unobtrusive Continuous Measurement of Autonomic Nervous System," *IEEE Internet of Things Journal*, vol. 6, no. 1, pp. 1104–1113, feb 2019.

[18] H.-G. Kim, E.-J. Cheon, D.-S. Bai, Y. H. Lee, and B.-H. Koo, "Stress and Heart Rate Variability: A Meta-Analysis and Review of the Literature," *Psychiatry Investigation*, vol. 15, no. 3, pp. 235–245, mar 2018.

[19] L. M. Vela, H. Kwon, S. B. Rutkove, and B. Sanchez, "Standalone IoT Bioimpedance Device Supporting Real-Time Online Data Access," *IEEE Internet of Things Journal*, vol. 6, no. 6, pp. 9545–9554, dec 2019.

[20] E. M. Spinelli, N. H. Martinez, and M. A. Mayosky, "A single supply biopotential amplifier," *Medical Engineering & Physics*, vol. 23, no. 3, pp. 235–238, apr 2001.

[21] T. Lim and H. Zhang, "Multilayer Carbon Nanotube/Gold Nanoparticle Composites on Gallium-Based Liquid Metals for Electrochemical Biosensing," *ACS Applied Nano Materials*, p. acsanm.1c03244, nov 2021.

[22] U. Kunzmann, G. von Wagner, J. Schöchlin, and A. Bolz, "Parameter extraction of ECG signals in real-time." *Biomedizinische Technik. Biomedical engineering*, vol. 47 Suppl 1, pp. 875–8, 2002.

[23] I. Iliev, V. Krasteva, and S. Tabakov, "Real-time detection of pathological cardiac events in the electrocardiogram." *Physiological measurement*, vol. 28, no. 3, pp. 259–76, mar 2007.

[24] S. Tabakov, I. Iliev, and V. Krasteva, "Online digital filter and QRS detector applicable in low resource ECG monitoring systems." *Annals of biomedical engineering*, vol. 36, no. 11, pp. 1805–15, nov 2008.

[25] W. C. Birmingham, L. L. Wadsworth, M. Hung, W. Li, and R. M. Herr, "Ambivalence in the Early Years of Marriage: Impact on Ambulatory Blood Pressure and Relationship Processes." *Annals of behavioral medicine : a publication of the Society of Behavioral Medicine*, vol. 53, no. 12, pp. 1069–1080, 2019.

[26] T. Cornelius, J. L. Birk, D. Edmondson, and J. E. Schwartz, "Ambulatory Blood Pressure Response to Romantic Partner Interactions and Long-Term Cardiovascular Health Outcomes." *Psychosomatic medicine*, vol. 82, no. 4, pp. 393–401, 2020.

[27] J. Holt-Lunstad, W. Birmingham, and B. Q. Jones, "Is there something unique about marriage? The relative impact of marital status, relationship quality, and network social support on ambulatory blood pressure and mental health." *Annals of behavioral medicine : a publication of the Society of Behavioral Medicine*, vol. 35, no. 2, pp. 239–44, apr 2008.

[28] J. Holt-Lunstad, W. A. Birmingham, and K. C. Light, "Influence of a "warm touch" support enhancement intervention among married couples on ambulatory blood pressure, oxytocin, alpha amylase, and cortisol." *Psychosomatic medicine*, vol. 70, no. 9, pp. 976–85, nov 2008.

[29] T. I. Burford, C. A. Low, and K. A. Matthews, "Night/day ratios of ambulatory blood pressure among healthy adolescents: roles of race, socioeconomic status, and psychosocial factors." *Annals of behavioral medicine : a publication of the Society of Behavioral Medicine*, vol. 46, no. 2, pp. 217–26, oct 2013.

[30] K. A. Matthews and L. C. Gallo, "Psychological perspectives on pathways linking socioeconomic status and physical health." *Annual review of psychology*, vol. 62, pp. 501–30, 2011.

[31] J. Holt-Lunstad, B. N. Uchino, T. W. Smith, C. Olson-Cerny, and J. B. Nealey-Moore, "Social relationships and ambulatory blood pressure: Structural and qualitative predictors of cardiovascular function during everyday social interactions." *Health Psychology*, vol. 22, no. 4, pp. 388–397, 2003.

[32] B. J. Lehman, A. C. Cane, S. J. Tallon, and S. F. Smith, "Physiological and emotional responses to subjective social evaluative threat in daily life." *Anxiety, stress, and coping*, vol. 28, no. 3, pp. 321–39, 2015.

[33] S. S. Brady and K. A. Matthews, "Effects of media violence on health-related outcomes among young men." *Archives of pediatrics & adolescent medicine*, vol. 160, no. 4, pp. 341–7, apr 2006.

[34] J. M. Cundiff, W. C. Birmingham, B. N. Uchino, and T. W. Smith, "Marital Quality Buffers the Association Between Socioeconomic Status and Ambulatory Blood Pressure." *Annals of behavioral medicine : a publication of the Society of Behavioral Medicine*, vol. 50, no. 2, pp. 330–5, apr 2016.

[35] R. L. Piferi and K. A. Lawler, "Social support and ambulatory blood pressure: an examination of both receiving and giving." *International journal of psychophysiology : official journal of the International Organization of Psychophysiology*, vol. 62, no. 2, pp. 328–36, nov 2006.

[36] B. N. Uchino, C. A. Berg, T. W. Smith, G. Pearce, and M. Skinner, "Age-related differences in ambulatory blood pressure during daily stress: evidence for greater blood pressure reactivity with age." *Psychology and aging*, vol. 21, no. 2, pp. 231–9, jun 2006.

[37] A. de Kock, L. Malan, M. Hamer, M. Cockeran, and N. T. Malan, "Defensive coping and renovascular disease risk - Adrenal fatigue in a cohort of Africans and Caucasians: The SABPA study." *Physiology & behavior*, vol. 147, pp. 213–9, aug 2015.

[38] C. Foody, J. E. James, and G. Leader, "Parenting Stress, Salivary Biomarkers, and Ambulatory Blood Pressure: A Comparison Between Mothers and Fathers of Children with Autism Spectrum Disorders," *Journal of Autism and Developmental Disorders*, vol. 45, no. 4, pp. 1084–1095, apr 2015.

[39] K. Bagot, S. Matthews, M. Mason, L. M. Squeglia, J. Fowler, K. Gray, M. Herting, A. May, I. Colrain, J. Godino, S. Tapert, S. Brown, and K. Patrick, "Current, future and potential use of mobile and wearable technologies and social media data in the ABCD study to increase understanding of contributors to child health," *Developmental Cognitive Neuroscience*, vol. 32, pp. 121–129, aug 2018.

[40] K. Barbaro, "Automated sensing of daily activity: A new lens into development," *Developmental Psychobiology*, vol. 61, no. 3, pp. 444–464, apr 2019.

[41] M. E. Morris and A. Aguilera, "Mobile, social, and wearable computing and the evolution of psychological practice." *Professional Psychology: Research and Practice*, vol. 43, no. 6, pp. 622–626, dec 2012.

[42] L. Menghini, E. Gianfranchi, N. Cellini, E. Patron, M. Tagliabue, and M. Sarlo, "Stressing the accuracy: Wrist-worn wearable sensor validation over different conditions," *Psychophysiology*, vol. 56, no. 11, nov 2019.

[43] N. Milstein and I. Gordon, "Validating Measures of Electrodermal Activity and Heart Rate Variability Derived From the Empatica E4 Utilized in Research Settings That Involve Interactive Dyadic States," *Frontiers in Behavioral Neuroscience*, vol. 14, aug 2020.

[44] W. Philips, "Adaptive noise removal from biomedical signals using warped polynomials," *IEEE Transactions on Biomedical Engineering*, vol. 43, no. 5, pp. 480–492, may 1996.

[45] A. Khaing, "Quantitative Investigation of Digital Filters in Electrocardiogram with Simulated Noises," *International Journal of Information and Electronics Engineering*, vol. 3, no. 3, pp. 210–216, 2011.

[46] G. G. Bernston and J. R. Stowell, "ECG artifacts and heart period variability: Don't miss a beat!" *Psychophysiology*, vol. 35, no. 1, pp. 127–132, jan 1998.

[47] A. Gibbs, M. Fitzpatrick, M. Lilburn, H. Easlea, J. Francey, R. Funston, J. Diven, S. Murray, O. G. J. Mitchell, A. Condon, A. R. J. Mitchell, B. Sanchez, and D. Steinhaus, "A universal, high-performance ECG signal processing engine to reduce clinical burden." *Annals of noninvasive electrocardiology : the official journal of the International Society for Holter and Noninvasive Electrocardiology, Inc*, p. e12993, jul 2022.

[48] H. Wu, G. Yang, K. Zhu, S. Liu, W. Guo, Z. Jiang, and Z. Li, "Materials, Devices, and Systems of On-Skin Electrodes for Electrophysiological Monitoring and Human–Machine Interfaces," *Advanced Science*, vol. 8, no. 2, p. 2001938, jan 2021.

[49] A. Lozano, J. Rosell, and R. Pallas-Areny, "Errors in prolonged electrical impedance measurements due to electrode repositioning and postural changes," *Physiological Measurement*, vol. 16, no. 2, pp. 121–130, may 1995.

[50] N. Meziane, J. G. Webster, M. Attari, and A. J. Nimunkar, "Dry electrodes for electrocardiography," *Physiological Measurement*, vol. 34, no. 9, pp. R47–R69, sep 2013.

[51] Y. M. Chi, T.-P. Jung, and G. Cauwenberghs, "Dry-contact and non-contact biopotential electrodes: methodological review." *IEEE reviews in biomedical engineering*, vol. 3, pp. 106–19, 2010.

[52] P. A. Lopes, D. Vaz Gomes, D. Green Marques, P. Faia, J. Góis, T. F. Patrício, J. Coelho, A. Serra, A. T. de Almeida, C. Majidi, and M. Tavakoli, "Soft Bioelectronic Stickers: Selection and Evaluation of Skin-Interfacing Electrodes," *Advanced Healthcare Materials*, vol. 8, no. 15, p. 1900234, aug 2019.

[53] T. Daeneke, K. Khoshmanesh, N. Mahmood, I. A. de Castro, D. Esrafilzadeh, S. J. Barrow, M. D. Dickey, and K. Kalantar-zadeh, "Liquid metals: fundamentals and applications in chemistry," *Chemical Society Reviews*, vol. 47, no. 11, pp. 4073–4111, 2018.

[54] M. D. Dickey, "Stretchable and Soft Electronics using Liquid Metals," *Advanced Materials*, vol. 29, no. 27, p. 1606425, jul 2017.

[55] T. Lim, M. Kim, A. Akbarian, J. Kim, P. A. Tresco, and H. Zhang, "Conductive Polymer Enabled Biostable Liquid Metal Electrodes for Bioelectronic Applications," *Advanced Healthcare Materials*, p. 2102382, feb 2022.

[56] T. Lim, T. A. Ring, and H. Zhang, "Chemical Analysis of the Gallium Surface in a Physiologic Buffer," *Langmuir*, may 2022.

[57] J.-H. Kim, S. Kim, J.-H. So, K. Kim, and H.-J. Koo, "Cytotoxicity of Gallium–Indium Liquid Metal in an Aqueous Environment," *ACS Applied Materials & Interfaces*, vol. 10, no. 20, pp. 17 448–17 454, may 2018.

[58] T. Lim and H. Zhang, "Multilayer Carbon Nanotube/Gold Nanoparticle Composites on Gallium-Based Liquid Metals for Electrochemical Biosensing," *ACS Applied Nano Materials*, vol. 4, no. 11, pp. 12 690–12 701, nov 2021.

[59] D. Burin, N. Yamaya, R. Ogitsu, and R. Kawashima, "Virtual training leads to real acute physical, cognitive, and neural benefits on healthy adults: study protocol for a randomized controlled trial," *Trials*, vol. 20, no. 1, p. 559, dec 2019.

[60] D. H. Gomez, J. R. Bagley, N. Bolter, M. Kern, and C. M. Lee, "Metabolic Cost and Exercise Intensity During Active Virtual Reality Gaming," *Games for Health Journal*, vol. 7, no. 5, pp. 310–316, oct 2018.

[61] M. Malińska, K. Zużewicz, J. Bugajska, and A. Grabowski, "Heart rate variability (HRV) during virtual reality immersion," *International Journal of Occupational Safety and Ergonomics*, vol. 21, no. 1, pp. 47–54, jan 2015.

[62] S. M. Peterson, E. Furuichi, and D. P. Ferris, "Effects of virtual reality high heights exposure during beam-walking on physiological stress and cognitive loading," *PLOS ONE*, vol. 13, no. 7, p. e0200306, jul 2018.

[63] D. Opris, S. Pintea, A. Garcia-Palacios, C. Botella, S. Szamoskozi, and D. David, "Virtual reality exposure therapy in anxiety disorders:

a quantitative meta-analysis," *Depression and Anxiety*, vol. 29, no. 2, pp. 85–93, feb 2012.

[64] S. García-Bravo, A. Cuesta-Gómez, R. Campuzano-Ruiz, M. J. López-Navas, J. Domínguez-Paniagua, A. Araújo-Narváez, E. Barreñada-Copete, C. García-Bravo, M. T. Flórez-García, J. Botas-Rodríguez, and R. Cano-de-la Cuerda, "Virtual reality and video games in cardiac rehabilitation programs. A systematic review," *Disability and Rehabilitation*, vol. 43, no. 4, pp. 448–457, feb 2021.

[65] S. Ahmed, M. Safdar, C. Morton, N. Soave, R. Patel, K. Castillo, S. Lalande, L. Jimenez, J. H. Mateika, and R. Wessells, "Effect of virtual reality-simulated exercise on sympathovagal balance," *PLOS ONE*, vol. 15, no. 7, p. e0235792, jul 2020.

[66] M. Wallergård, P. Jönsson, G. Johansson, and B. Karlson, "A Virtual Reality Version of the Trier Social Stress Test: A Pilot Study," *Presence: Teleoperators and Virtual Environments*, vol. 20, no. 4, pp. 325–336, aug 2011.

[67] B. Sanchez, O. G. Martinsen, T. J. Freeborn, and C. M. Furse, "Electrical impedance myography: A critical review and outlook," *Clinical Neurophysiology*, vol. 132, no. 2, pp. 338–344, feb 2021.

[68] B. Sanchez and S. B. Rutkove, "Electrical Impedance Myography and Its Applications in Neuromuscular Disorders," *Neurotherapeutics*, vol. 14, no. 1, pp. 107–118, jan 2017.

[69] S. S. Gill, M. Xu, C. Ottaviani, P. Patros, R. Bahsoon, A. Shaghaghi, M. Golec, V. Stankovski, H. Wu, A. Abraham, M. Singh, H. Mehta, S. K. Ghosh, T. Baker, A. K. Parlikad, H. Lutfiyya, S. S. Kanhere, R. Sakellariou, S. Dustdar, O. Rana, I. Brandic, and S. Uhlig, "AI for next generation computing: Emerging trends and future directions," *Internet of Things*, vol. 19, p. 100514, aug 2022.

Luis M. Vela received his M.Sc. degree in electrical engineering from Universitat Politecnica de Catalunya (UPC), Barcelona, Spain. In 2015 he obtained a Certified SCRUM Master certification from Agilar.

He has been devoted to the development of embedded software (SW) systems for the last 20 years. Specialized in time and safety critical systems development, he has worked in several sectors including telecom, banking, automotive and aerospace. His main interest are critical SW analysis, design, development and validation following safety critical norms (i.e. ISO15504, ISO62626, ECCS) and agile SW methodologies.

Henry Crandall received a B.S. degree in electrical engineering with the highest honors from the University of Utah in 2021. Henry is currently an ARCS Scholar pursuing a Ph.D. in electrical engineering at the same institution with an emphasis in bioimpedance. His research focuses on developing wearable health monitors.

Taehwan Lim received the B.S. degree in molecular system engineering from the Hanyang University, Seoul, South Korea, and the M.S. degree in organic and nano engineering from the Hanyang University, Seoul, South Korea, in 2012. He joined the Korea Institute of Industrial Technology (KITECH) from 2012 to 2016 and worked on conductive material composites and carbon fiber preparation. He also received a Ph.D. degree in chemical engineering from the University of Utah, Salt Lake City, UT, USA, focusing on Gallium core-shell microstructure for thermal responsive implantable neural electrodes. Now, he works at the Korea Institute of Industrial Technology (KITECH) as a Post-Doc. His research interests include flexible and stretchable electronics, biomedical materials, metal surface chemistry, functional fiber technology, and electrochemistry.

Fu Zhang received the B.S. and M.S. degrees in Measuring & Control Technology and Instrumentation from Xi'an University of Technology, Shaanxi, China in 2012 and 2015, respectively, and the Ph.D. degree in Hunan University, Hunan, China in 2020. He was a visiting scholar in the Department of Neurology, Beth Israel Deaconess Medical Center–Harvard Medical School, MA, USA from 2017-2019. He is now instructor in Department of Electronics, Hunan Normal University, Hunan, China. His research focuses on developing novel bioimpedance measuring and modeling technologies for health management and biomedical monitoring. He has published 12 co-authored articles in peer-reviewed international journals, including Physiological Measurement, IEEE Transactions on Instrumentation and Measurement, IET Science, Measurement & Technology, Circuits, Systems, and Signal Processing.

Austin Gibbs Dr graduated from University College London with degrees in Medicine and Psychology and has worked in Emergency Medicine and on healthcare projects in various settings across the world. Founded Mobile Medics, a charitable organisation supporting projects in remote Africa, drove from London to Johannesburg setting clinics in South Sudan and Limpopo in Mozambique. Set up the Jersey Research Foundation, a local charity that helps facilitate and empower residents to pursue scientific research and further education.

Currently, he is implementing Software as A Service AI diagnostic programs, remote patient monitoring, electronic consent and Virtual reality simulation training in Jersey.

Andrew R. J. Mitchell is Consultant Cardiologist at Jersey General Hospital and Honorary Consultant at Oxford University Hospitals. His research programme focusses on the development and application of digital health technologies to enhance clinical care.

Adrian Condon has significant experience and track record in new product design, leading technical teams and delivering strategic new technology across the industrial, automotive, aeronautical and medical industries.

Lisa M. Diamond is Professor of Psychology and Gender Studies at the University of Utah. For over 25 years, she has studied the development and expression of gender and sexuality across the life course. Her current work focuses on the biobehavioral mechanisms through which social stigma, social stress, and social safety shape the health and well-being of sexually-diverse and gender-diverse individuals at different stages of development. Dr. Diamond is best known for her research on sexual fluidity, which describes the capacity for individuals to experience unexpected shifts in sexual identity and expression over time. Her 2008 book, Sexual Fluidity, published by Harvard University Press, has been awarded the Distinguished Book Award from the American Psychological Association's Society for the Study of LGBTQ Issues. Dr. Diamond is also co-editor of the first-ever APA Handbook of Sexuality and Psychology, published in 2014, and is a fellow of two divisions of the APA. She has published over 130 articles and book chapters, and has been invited to present her research at nearly 140 national and international Universities and conferences. Dr. Diamond has received awards for her work from the Developmental Psychology and LGBT Psychology Divisions of the APA, the Society for Personality and Social Psychology, the International Association for Relationship Research, the Society for the Scientific Study of Sexuality, and the Society for the Psychological Study of Social Issues.

Huanan Zhang received the B.S. degree in chemical-biological engineering from the Massachusetts Institute of Technology, Cambridge, MA, USA, and the Ph.D. degree in chemical engineering from the University of Michigan, Ann Arbor, MI, USA, in 2014 with a focus on electrochemical/material neural interface. He is an Assistant Professor of chemical engineering. He has extensive experience in electrochemistry of the biological system, material synthesis/design for implantable electronics, and in vitro/in vivo device validation.

Benjamin Sanchez Terrones (M'13-SM'20), received a dual B.S. degree in Telecommunication and Electronic Engineering, and the M.S, and Ph.D. degrees in Electronic Engineering from Universitat Politecnica de Catalunya (UPC), Barcelona, Spain, in 2006, 2007, 2008, and 2012, respectively.

He was a Visiting Scholar in the Department of Fundamental Electricity and Instrumentation, Vrije Universiteit Brussel, Brussels, Belgium, and the Department of Automatic Control, School of Electrical Engineering, Royal Institute of Technology (KTH), Stockholm, Sweden, in 2012 and 2013, respectively. From 2014−2020, he was Instructor in Neurology at Beth Israel Deaconess Medical Center, Harvard Medical School, Boston, MA, USA. Since 2020, he has been an Assistant Professor of Electrical and Computer Engineering at the University of Utah and Member of the Huntsman Cancer Institute, Salt Lake City, UT, USA. His research focuses on developing novel technologies for measuring and monitoring health.

Dr. Sanchez has co-authored 80 articles published in physics, medicine and engineering journals, 1 book chapter, and has 4 issued and 2 pending patents. His research has been Highlighted by the journals MEASUREMENT SCIENCE & TECHNOLOGY in 2012, PHYSIOLOGICAL MEASUREMENT in 2013, 2015 and 2017, CLINICAL NEUROPHYSIOLOGY in 2020 and 2021, HEART RHYTHM in 2023. He was the recipient of the 2012 Ph.D. Extraordinary Prize, Martin Black prize for the Best Paper Award in PHYSIOLOGICAL MEASUREMENT journal in 2014 for his bioimpedance work, winner of the President's Research Initiative Award from the American Association of Neuromuscular & Electrodiagnostic Medicine in 2014 and 2016. Dr. Sanchez serves as Associate Editor of IEEE JOURNAL OF ELECTROMAGNETICS, RF AND MICROWAVES IN MEDICINE AND BIOLOGY, and PHYSIOLOGICAL MEASUREMENT, and he is Editorial Board Member of IEEE OPEN JOURNAL OF ENGINEERING IN MEDICINE AND BIOLOGY.